

SHARP BOUNDARY INVERSION OF TENSOR INDUCTION LOGGING DATA

Michael S. Zhdanov*, Arvidas B. Cheryauka, and Ertan Peksen

Department of Geology and Geophysics, University of Utah, Salt Lake City, Utah 84112

ABSTRACT

In this paper we develop and analyze a new technique for interpretation of the tensor induction well logging (TIWL) data. This method, which we call *sharp boundary inversion*, is based on using specially selected stabilizing functionals, which minimize the area where strong model parameter variations and discontinuity occur. The method recovers the sharp boundary between different anisotropic geoelectrical layers and reconstructs both the horizontal and vertical resistivity profiles. The developed algorithm was tested by interpreting the synthetic TIWL data collected with a typical tensor induction tool in a deviated well in the layered anisotropic formations.

INTRODUCTION

The horizontally layered formation with anisotropy in electric conductivity properties is an important interpretation model for evaluating oil and gas bearing reservoirs (Moran and Gianzero, 1979; Yin, 2000). Induction well logging in anisotropic formations has recently become an area of active research and industrial development. A number of papers discussing a multi-component induction logging tool were published during the last several years (Kriegshauser et al. 2000a,b; Zhdanov et al., 2001a,b). At the same time, even the interpretation of data, collected by the conventional induction devices in stratified formations and deviated wells, is a complicated task due to existing limitations in the observation systems and data processing techniques (Gupta et al., 1998, 1999; Barber et al., 1999; Kriegshauser et al., 2000b). One of the problems of the layered model inversion is related to the fact, that the majority of existing inversion algorithms tends to produce a smooth distribution of the electric conductivity, while the real layered formations are characterized by the sharp resistivity contrasts between the different layers. The efficient algorithms for blocking resistivities in well-logging interpretation have been proposed in Chouinard and Paulson (1988) and Qian and Zhong (1999). They have simplified the delineation of formation's interfaces and significantly reduced the data processing expenses by grouping the thin beds of close properties.

In this paper we develop and analyze a new technique for interpretation of the tensor induction well logging (TIWL) data in a horizontally layered formation. The goal of interpretation is to find the layer's

interfaces and conductivities. However, the solution of this problem meets a lot of difficulties even for the case of conventional induction logging in an isotropic layered formation. The problem is that the traditional inversion methods use the smooth models of conductivity distribution along the borehole to provide a stable and reliable solution. However, in the layered formation the conductivity changes sharply when we cross the layer's boundaries. In this case a smooth model does not represent well the real physical properties of the medium. Cheryauka and Zhdanov (2001b) proposed to use in the inversion of the induction logging data a new approach of focusing inversion developed by Portniaguine and Zhdanov (1999) for gravity data interpretation. This approach, which we call *sharp boundary inversion*, is based on using specially selected stabilizing functionals, which minimize the area where strong model parameter variations and discontinuity occur. In the current paper we present the principles and preliminary modeling results for inversion of tensor induction well-logging data in the layered anisotropic formations based on focusing stabilizing functionals and the re-weighted regularized conjugate gradient method (Zhdanov, 2002).

FORMULATION OF THE INVERSE PROBLEM

The inverse problem is formulated for TIWL data collected in a deviated borehole within a planar stratified medium with electrical anisotropy in each layer. We assume that a model of the horizontally layered medium is characterized in the coordinate system $\{x, y, z\}$ by 1-D piecewise-constant distribution of the conductivity along the z direction. Each layer has transverse isotropic conductivity defined by a conductivity tensor $\hat{\sigma}_i(z)$

$$\hat{\sigma}_i = \begin{pmatrix} \sigma_{hi} & 0 & 0 \\ 0 & \sigma_{hi} & 0 \\ 0 & 0 & \sigma_{vi} \end{pmatrix}, \quad (1)$$

and the corresponding piecewise constant anisotropy coefficient

$$\lambda_i = (\sigma_{hi}/\sigma_{vi})^{1/2}, \quad i=1, \dots, N. \quad (2)$$

The positions of the layer's boundaries are given by equations

$$z = z_i, \quad i=1, \dots, N-1. \quad (3)$$

PP

The ideal tensor induction well logging tool detects three components of the magnetic field due to each of three transmitters for a total of nine signals, which form the induction tensor:

$$\widehat{\mathbf{H}}' = \begin{bmatrix} H_{x'}^{x'} & H_{x'}^{y'} & H_{x'}^{z'} \\ H_{y'}^{x'} & H_{y'}^{y'} & H_{y'}^{z'} \\ H_{z'}^{x'} & H_{z'}^{y'} & H_{z'}^{z'} \end{bmatrix},$$

where $\{x', y', z'\}$ is the instrument coordinate system with the z' - axes coinciding with the tool and borehole lines, and the y - and y' - axes being mutually parallel as proposed in Zhdanov et al. (2001a); the superscripts indicate the transmitter components and subscripts represent the receiver components.

In the framework of a 1-D interpretation model we ignore the borehole and invasion zone effects (Gupta et al., 1998, 1999; Barber et al., 1999), assuming that these effects can be excluded by multi-frequency observations. We also assume that we know the dip angle α between the vertical z -axes of the medium coordinate system (perpendicular to the layer interfaces) and the z' -axes of the instrument coordinate system (the borehole trajectory), and the rotation position of the tensor tool in the $x'y'$ - plane of the instrument coordinate system with respect to the axis xy of the medium coordinate system, characterized by the relative bearing angle β . Actually, this information can be obtained from the tensor induction tool data itself (Zhdanov et al., 2001a,b, Peksen and Zhdanov, 2002), but in this study we assume that α is known and $\beta = 0$ (the y and y' axes coincide, i.e. there is no rotation in the $x'y'$ - plane). In the instrument coordinate system introduced above, the tool measures the following four components of the induction tensor,

$$\{H_{x'}^{x'}, H_{y'}^{y'}, H_{z'}^{z'}, H_{z'}^{x'}\}.$$

Following the conventional practice in well-logging inversion, we represent a layered formation as a set of sample layers with a given small thickness Δh (see, for example, Barber et al., 1999). Thus, we reduce the inverse problem to determining the resistivities of the sample layers only.

The TIWL inverse problem can be formulated as the solution of the operator equation

$$\mathbf{d} = \mathbf{A}(\mathbf{m}), \quad (4)$$

where the data vector \mathbf{d} is formed by the tensor components $H_{x'}^{x'}, H_{y'}^{y'}, H_{z'}^{z'}, H_{z'}^{x'}$ observed by the TIWL

tool in the deviated well, the vector \mathbf{m} of the model parameter distributions consists of the logarithms of the horizontal and vertical conductivities, $(\ln \sigma_{hi}$ and $\ln \sigma_{vi}, i=1, \dots, M)$ of the sample layers forming a 1-D geoelectrical inverse model,

$$\mathbf{m} = [\ln \sigma_{h1}, \ln \sigma_{v1}, \ln \sigma_{h2}, \ln \sigma_{v2}, \dots, \ln \sigma_{hM}, \ln \sigma_{vM}]$$

where M is the number of the sample layers. The induction logging inverse problem consists in finding a distribution of the model parameters \mathbf{m} which corresponds to the observed discrete set of the tensor induction data \mathbf{d} .

SHARP BOUNDARY INVERSION METHOD

The solution of this problem, as for the most geophysical inverse problems, is a non-unique and ill-posed. Following the basic principles of the regularization theory (Tikhonov and Arsenin, 1977; Zhdanov, 2002), we solve this ill-posed inverse problem by minimization of the corresponding parametric functional:

$$P^\alpha(\mathbf{m}) = \phi(\mathbf{m}) + \nu s(\mathbf{m}) = \min, \quad (5)$$

where $\phi(\mathbf{m})$ is the misfit, $s(\mathbf{m})$ is the stabilizing functional, and ν is a regularization parameter.

We specify the misfit functional as

$$\phi(\mathbf{m}) = \left\| \widehat{\mathbf{W}}_d (\widehat{\mathbf{A}}\mathbf{m} - \mathbf{d}) \right\|_{L_2}^2, \quad (6)$$

where $\widehat{\mathbf{W}}_d$ is the data weighting matrix.

Following the general method of sharp boundary inversion (Portniaguine and Zhdanov, 1999; Zhdanov, 2002), we select the minimum gradient support stabilizing functional, which minimizes the area where the variations of the vertical and horizontal conductivities occur:

$$s(\mathbf{m}) = s_{MGS}(\mathbf{m}) = \left\| \frac{|\nabla \mathbf{m}|}{(|\nabla \mathbf{m}|^2 + e^2)^{1/2}} \right\|_{L_2}^2, \quad (7)$$

where e is a small number introduced to exclude a singularity at zero gradient. This functional is designed to increase the resolution of the blocky model structures.

In numerical calculations we represent the model parameter function m by a vector \mathbf{m} formed by the

logarithms of the horizontal and vertical conductivities of the layers $\{\ln \sigma_{h,j}, \ln \sigma_{v,j}\}$, $j=1, \dots, M$. We introduce also the $(2M \times 2M)$ matrix $\widehat{\mathbf{L}}$ of the vertical gradient operator with only two non-zero diagonals

$$\widehat{\mathbf{L}} = \begin{bmatrix} 1 & 0 & \dots & 0 & 0 \\ -1 & 1 & \dots & 0 & 0 \\ \dots & \dots & \dots & \dots & \dots \\ 0 & 0 & \dots & 1 & 0 \\ 0 & 0 & & -1 & 1 \end{bmatrix}.$$

We modify the expression (7) for discrete model parameters and, following Zhdanov (2002), represent a stabilizing functional in the form of the pseudo-quadratic functional:

$$s_{MGS}(\mathbf{m}) = \left\| \left(\widehat{\mathbf{L}}\mathbf{m} \right)^T \widehat{\mathbf{W}}_e^{-2} \left(\widehat{\mathbf{L}}\mathbf{m} \right) \right\|_{L_2(M)}, \quad (8)$$

where superscript “**T**” means the transposition. The matrix multiplication $\widehat{\mathbf{L}}\mathbf{m}$ describes the finite difference derivation of the vector \mathbf{m} of the discrete model parameters. The variable weighting matrix $\widehat{\mathbf{W}}_e$ for the s_{MGS} functional, according to Zhdanov, 2002, is given by the formula

$$\widehat{\mathbf{W}}_e = \text{diag}[|\nabla\mathbf{m}|^2 + e^2]^{1/2} = \left[\text{diag}^2 \left(\widehat{\mathbf{L}}\mathbf{m} \right) + e^2 \widehat{\mathbf{I}} \right]^{1/2} \quad (9)$$

where symbol $\text{diag} \left[\widehat{\mathbf{L}}\mathbf{m} \right]$ denotes a diagonal matrix with the diagonal elements formed by the components of the vector $\widehat{\mathbf{L}}\mathbf{m}$, e is a small number introduced to exclude a singularity in expression (8), and $\widehat{\mathbf{I}}$ is identity matrix.

We solve the minimization problem (5) using the re-weighted regularized conjugate gradient method (Zhdanov, 2002).

INVERSION OF THE SYNTHETIC TIWL DATA

In practical application of the developed inversion method, we apply the inversion first to find the 1-D horizontal conductivity model, and after that, we invert for the vertical conductivity model. This approach can be justified based on the following consideration. The tri-axial electromagnetic induction well-logging instrument measures all components of the induction tensor (Zhdanov et al., 2001a). These measurements allow us, in principle, to separate the toroidal (TM) and poloidal (TE) modes of the EM field generated in the 1-D model (Berdichevsky and

Zhdanov, 1984; Cheryauka and Zhdanov, 2001a). The toroidal mode, TM, contains only tangential components of electromagnetic field with respect to the layer interfaces. The poloidal mode, TE, contains not only tangential components but a vertical (perpendicular to the layer interfaces) component as well. Computing the vertical magnetic field response in the medium coordinate system from the tensor induction data, we separate a poloidal portion of the signal, which depends on the distribution of the horizontal conductivities of the layers only. So, in the first stage of the inversion procedure we restore the horizontal conductivities of the layers. As an initial guess we use the apparent conductivities, which are computed by fitting the observed signal with the theoretical response from the unbounded homogeneous space of an optimal resistivity (Zhdanov et al., 2001b). We minimize the parametric functional P^α in (5) with the focusing stabilizer (8) using the re-weighted conjugate gradient method (Zhdanov, 2002) until the misfit functional becomes less than the noise level.

The resultant horizontal conductivity distribution may serve as an initial guess in the second stage of inversion, namely, for the vertical conductivity inversion. However, we can chose the apparent vertical conductivity as the initial vertical conductivity distribution, as well. We apply the same iterative solver to determine the vertical conductivity cross-section, keeping the fixed values of the horizontal conductivities of the layers. In this stage we use the synthetic vector of the response H_x^x (the horizontal magnetic field from the horizontal magnetic dipole in the medium coordinate system) for the inversion, because this component contains the toroidal mode of the field, which is sensitive to the vertical conductivity. The component H_x^x in the medium coordinate system can be computed from the observed tensor components $H_{x'}^{x'}$, $H_{y'}^{y'}$, $H_{z'}^{z'}$, $H_{z'}^{x'}$ in the instrument coordinate system by applying the corresponding rotation matrix (Zhdanov, et al., 2001a).

We present several examples of inverting the responses of a tensor induction tool in the models of the layered TI formations. The configuration of an elementary tensor induction tool is shown in Figure 1. The transmitter receiver separation is 1.0 m. The moments of all tool magnetic dipoles are equal to 1 Am², and the operational frequency is 20 kHz. The dip angle of the borehole is equal to 30 degrees with respect to the vertical axes. For inversion, we represent each model as a set of the sample layers with a given small thickness $\Delta h = 40$ cm.

PP

The first example represents a simple two layered anisotropic model 1 (Figures 2 and 3). The relative deviation angle between a borehole and the axis of symmetry of the transverse isotropic medium is equal to 30 degrees. This angle may be determined from the TIWL data using low frequency asymptotics (Zhdanov et al., 2001a), therefore, we assume that the relative deviation angle is known. The left frame in Figure 2 shows the true horizontal resistivity of model 1 (the solid line) and the initial guess based on the low frequency apparent resistivity calculation (the dotted-solid line). The synthetic measured data have been calculated using the GT3D software (Cheryauka and Zhdanov, 2001a) and contaminated by 3% white noise. The right frame in the same figure demonstrates the data observed and predicted by inversion (“+” and “-” symbols show the real and imaginary parts of observed data H_z^z , respectively, while the “.” and “_” symbols show the real and imaginary parts of the predicted data H_z^z). The field in air is subtracted from in-phase parts of the signals. The final inversion result for the horizontal resistivity is shown by the circles in the left panel of Figure 2. We use the obtained distribution of the horizontal resistivities as a starting model for the vertical resistivity inversion (Figure 3, the left frame). The resulting model of the vertical resistivity distribution is shown in Figure 3, left panel, by the circles. The right panel in this figure demonstrates how well the predicted data fit the observed data H_x^x . We can see in these figures that the true resistivity profiles are recovered quite well with the sharp boundary inversion.

In the next Figures 4 and 5, we present the inversion results for a three-layered transverse anisotropic model 2. We choose the following parameters of the model: horizontal resistivity of the layers is equal to 3, 20, and 8 Ohm-m, while the vertical resistivity is of 6, 100, and 16 Ohm-m, respectively. We use the same notations for the different curves plotted in these figures, as in Figures 2 and 3. We observe again a good recovery of the true model resistivity profiles from the TIWL data.

In the next model test we analyze the Baker Atlas benchmark model (BA model, Yu et al., 2001). The authors of the cited paper inverted the synthetic multicomponent induction data generated for this model by Schon et al., 1999. The model comprises a sequence of the anisotropic layers with the different horizontal and vertical resistivities. We slightly modified this model to construct a formation consisting of seven sections with a thickness of two meters

each. We use the following parameters of the model:

horizontal resistivities of the layers - 1, 1.85, 2.59, 7.64, 20.00, 124.90, and 37.60 Ohm-m;

vertical resistivities - 2, 6.75, 8.67, 9.00, 31.25, 195.50, and 166.5 Ohm-m.

We represent this formation as a set of the sample layers with a given small thickness $\Delta h = 25$ cm. The synthetic tensor induction well logging (TIWL) data have been computed for the anisotropic BA model using the GT3D software developed by CEMI (Cheryauka and Zhdanov, 2001a). These data were processed using the inversion scheme outlined above. Figures 6 and 7 present the results of TIWL data interpretation for the anisotropic BA model. The results obtained with the focusing inversion algorithm show good restoration of the blocky resistivity profiles in anisotropic formations. The horizontal resistivity images match precisely the piecewise geometry and electric properties of the layered structure. The images of vertical resistivity cross-section are slightly contaminated by the jumps that happened in the vicinities of the high-contrast layer boundaries. Note that the distortions are stronger at the ends of the induction log, and much smaller in the middle of the log.

As the final example we consider the, so-called, Oklahoma benchmark model (Barber et al. 1999), which is widely used for testing modeling codes in well-logging (Figure 8 the left frame). The original isotropic Oklahoma model consists of 27 high resistivity contrast layers with varying thicknesses from 0.3 m up to infinity (the unbounded half-space). We extend this model to anisotropic one, with the horizontal resistivities equal to the resistivities of the original Oklahoma model, and with the different vertical resistivities in 13 of 27 layers. The relative deviation angle between a borehole and the axis of symmetry of the transverse isotropic medium is equal to 30 degrees. The synthetic tensor induction well logging (TIWL) data have been computed for the anisotropic Oklahoma model using the GT3D software. These data were contaminated by 3% white noise and processed using the same inversion scheme outlined above.

Figures 8-10 present the results of TIWL data interpretation for the anisotropic Oklahoma model. The left frame in Figure 8 shows the true horizontal resistivity model (the solid line) and the initial guess based on the apparent resistivity calculation (the dotted line). The thickness of the sample layer is 0.5 m. The right frame in the same Figure demonstrates the measured (the solid and dotted lines for quadra-

ture and in-phase components, respectively) and the predicted (the circle markers) data for $MzHz$ tool configuration (the H_z' induction tensor component). The field in air is subtracted from in-phase parts of the signals. Figure 9 shows the final result of sharp boundary inversion for the horizontal resistivity (the dotted line) and the corresponding measured and predicted data. We use the obtained distribution of the horizontal resistivities as a starting model for the vertical resistivity inversion, and observe the horizontal magnetic field from the horizontal magnetic dipole (the H_x' induction tensor component) shown in Figure 10 (the right frame). The resulting model of the vertical resistivity distribution is shown in Figure 10 (the left panel). The results obtained with the sharp boundary inversion algorithm show good restoration of the blocky resistivity profiles in anisotropic formations. The horizontal resistivity images match precisely the piecewise geometry and electric properties of the layered structure. The images of vertical resistivity cross-section are slightly contaminated by the jumps happened in the vicinities of the high-contrast layer boundaries. These distortions can be decreased by applying a penalization of the anisotropy coefficient function to keep it within a range of [1 – 3], typical for real anisotropic formations.

CONCLUSIONS

We developed a method of TIWL data interpretation in the layered anisotropic formation. The method is based on regularized focusing inversion with the minimum gradient support stabilizer. This method recovers the sharp boundary between the different anisotropic geoelectrical layers and reconstructs both the horizontal and vertical resistivities profiles. We use the low frequency asymptotic formulae for the apparent horizontal and vertical resistivities of the tool as the initial model for inversion, which ensures the rapid convergence of the method. The developed algorithm was tested on the synthetic TIWL data collected by a typical multicomponent induction tool in the vertical and deviated wells in the layered anisotropic formations, including anisotropic Baker Atlas benchmark model and anisotropic Oklahoma model. The modeling results illustrate the practical effectiveness of this technique.

ACKNOWLEDGMENTS

The authors acknowledge the support of the University of Utah Consortium for Electromagnetic

Modeling and Inversion (CEMI), which includes Baker Atlas Logging Services, BHP Billiton World Exploration Inc., Electromagnetic Instruments, Inc., ExxonMobil Upstream Research Company, INCO Exploration, International Energy Services, Japan National Oil Corporation, MINDECO, Naval Research Laboratory, Rio Tinto-Kennecott, Shell International Exploration and Production Inc., Schlumberger Oilfield Services, and Sumitomo Metal Mining Co.

REFERENCES

- Barber, T. D., Broussard, T., Minerbo, G. N., Sijercic, Z., and D. Murgatroud, 1999, Interpretation of multiarray induction logs in invaded formations at high relative dip angles, *The Log Analyst*, **40**, no.3, 202-217.
- Berdichevsky, M. N., and M. S. Zhdanov, 1984, *Advanced theory of deep geomagnetic sounding: Elsevier, Amsterdam - New York - Tokyo*, 408 pp.
- Cheryauka, A. B., and M. S. Zhdanov, 2001a, Electromagnetic tensor Green's functions and their integrals in transversely isotropic layered media: *Proceedings of the CEMI Annual meeting*, 37-82.
- Cheryauka, A. B., and M. S. Zhdanov, 2001b, Focusing inversion of tensor induction logging data in anisotropic formations and deviated well: *Proceedings of the CEMI Annual meeting*, 289-312.
- Chouinard, P. N., and K. V. Paulson, 1988, A Markov-Gauss algorithm for blocking well logs: *Geophysics*, **53**, No. 4, 1118-1121.
- Gupta, P., Kriegshauser, B., Jericevic, Z., and O. Fanini, 1998, Method for inversion processing of transverse electromagnetic induction well logging measurements: *United States Patent 5,999,883*.
- Gupta, P., Kriegshauser, B., and O. Fanini, 1999, Conductivity anisotropy estimation method for inversion processing of measurements made by a transverse electromagnetic induction logging instrument: *United States Patent 5,854,991*.
- Kriegshauser, B. F., Fanini, O. N., Forgang, S., Itskovich, G., Rabinovich, M., Tabarovsky L., Epov, M., Gupta, and J. and D. Horst, 2000a, A new multicomponent induction tool to resolve anisotropic formations: *Proc. of SPWLA 69th Annual Meeting*, Calgary, paper D.
- Kriegshauser, B. F., Fanini, O. N., Yu, L., and P. K. Gupta, 2000b, Advanced inversion techniques for multicomponent induction log data: *Proc. of SEG 69th Annual Meeting*, Calgary, paper D.
- Moran, J. H., and S. Gianzero, 1979, *Effects of*

PP

formation anisotropy on resistivity-logging measurements: *Geophysics*, **44**, 1266-1286.

Peksen E., and M. S. Zhdanov, 2002, Apparent resistivity correction for tensor induction well logging in a deviated well in an anisotropic medium: Proceedings of the CEMI Annual meeting, 85-121.

Portniaguine, O., and M. S. Zhdanov, 1999, Focusing geophysical inversion images: *Geophysics*, **64**, No. 3, 874-887.

Qian, Y., and X. Zhong, 1999, Thin bed information resolution of well-logs and its applications; *The Log Analyst*, **40**, No. 1, 15-23.

Schon, J. H., Mollison, R. A., and D. T. Georgi, 1999, Macroscopic electrical anisotropy of laminated reservoir: A tensor resistivity tensor model: SPE 56509, in SPE Annual Technical Conference and Exhibition Transactions.

Tikhonov, A. N., and V. Y. Arsenin, 1977, Solution of ill-posed problems: Wilson & Sons, 258 pp.

Yu, L., Fanini, O. N., Kriegshauser, B. F., Koelman, J. M. V., and J. van Popta, 2001, Enhanced evaluation of low-resistivity reservoirs using multi-component induction log data: *Petrophysics*, **42**, No. 6, 611-623.

Yin, C., 2000, Geoelectrical inversion for a one-dimensional anisotropic model and inherent non-uniqueness: *Geophys. J. Inter.*, **140**, 11-23.

Zhdanov, M. S., Kennedy, W. D., and E. Peksen, 2001a, Foundations of tensor induction well-logging: *Petrophysics*, **42**, No. 6, 588-610.

Zhdanov, M. S., Kennedy, W. D., Cheryauka, B. A. and E. Peksen, 2001b, Principles of tensor induction well logging in a deviated well in an anisotropic medium: Transactions, 42-nd SPWLA Annual Logging Symposium, Houston, paper R.

Zhdanov, M. S., 2002, Geophysical inverse theory and regularization problems: Elsevier, Amsterdam, London, New York, Tokyo, 628 pp.

ABOUT THE AUTHORS

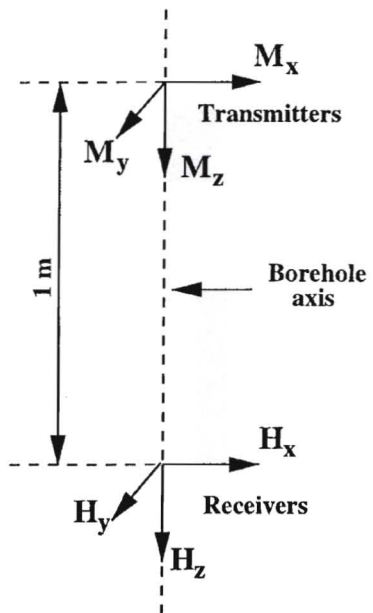
Michael S. Zhdanov is Professor of Geophysics, Director of the Consortium for Electromagnetic Modeling and Inversion (CEMI) at the University of Utah since 1993. He received PhD in physics and mathematics in 1970 from Moscow State University.

He was previously the Director of the Geoelectromagnetic Research Institute of the Russian Academy of Sciences, Moscow. In 1990 he was awarded an Honorary Diploma of Gauss Professor by the Gettingen Academy of Sciences, Germany. In 1991 he

was elected full member of the Russian Academy of Natural Sciences, in 1997 he became an Honorary Professor of China National Center of Geological Exploration Technology, and in 2002 he became a member of the Electromagnetic Academy, USA. His research interests are forward and inverse problems in geophysics. He is the author of more than 300 papers, including ten monographs.

Arvidas B. Cheryauka received his M.Sc. in Geophysics from the Novosibirsk State University, Russia in 1986 and a Ph.D in Geophysics from Institute for Geophysics, Siberian Branch of Russian Academy of Sciences in 1989. From 1995-1998 he worked as a consultant for LOOCH Geophysical Engineering and Baker Atlas companies. During 1998-1999, Arvidas was a visiting scientist with Tohoku University in Sendai, Japan. Since 1999 he has been working as a research scientist with Consortium for Electromagnetic Modeling and Inversion, University of Utah on the development of new array technologies for subsurface and well-logging sensing.

Ertan Peksen is a PhD student at the Consortium for Electromagnetic Modeling and Inversion, the University of Utah. He graduated in 1993 (BS) from the University of Ankara, in geophysics. He received his Master of Science degree in geophysics from the Department of Geology and Geophysics, the University of Utah, in 1999. His research interest is modeling and inversion of tensor induction well logging in anisotropic media.



PP

Figure 1: Tensor induction instrument with three mutually orthogonal transmitters and a triple of mutually orthogonal receivers located at a distance of 1 m from the transmitters.

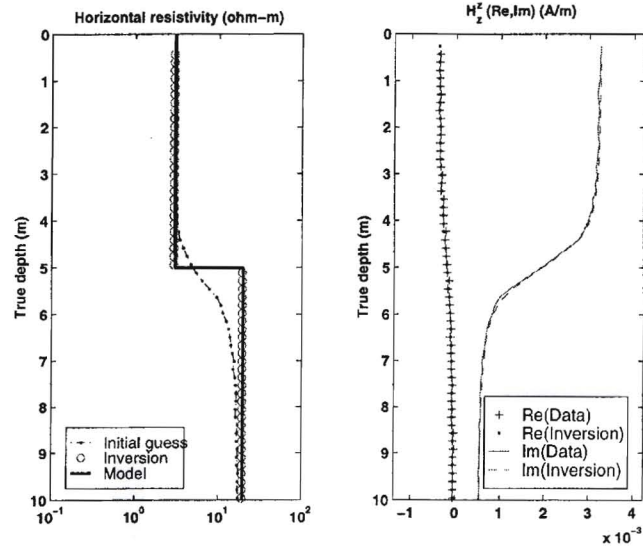


Figure 2: A two layered anisotropic model 1 with a deviated borehole ($\alpha = 30^\circ$). The solid line in the left panel represents a true model of the horizontal resistivity. The circles display the inversion result. The dotted-solid line describes the initial approximation. In the right panel we present the real and imaginary parts of the observed and predicted data H_z^z .

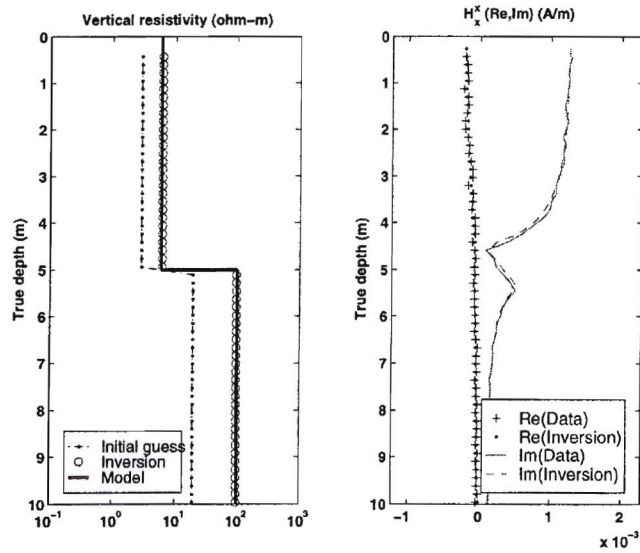


Figure 3: A two layered anisotropic model 1 with a deviated borehole ($\alpha = 30^\circ$). The solid line in the left panel represents a true model of the vertical resistivity. The circles display the inversion result. The dotted-solid line describes the initial approximation. In the right panel we present the real and imaginary parts of the observed and predicted data H_x^x .

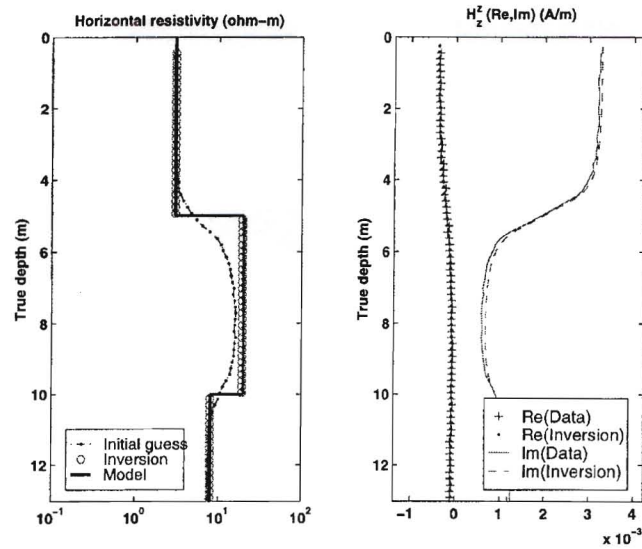


Figure 4: A three layered anisotropic model 2 with a deviated borehole ($\alpha = 30^\circ$). The solid line in the left panel represents a true model of the horizontal resistivity. The circles display the inversion result. The dotted-solid line describes the initial approximation. In the right panel we present the real and imaginary parts of the observed and predicted data H_z^2 .

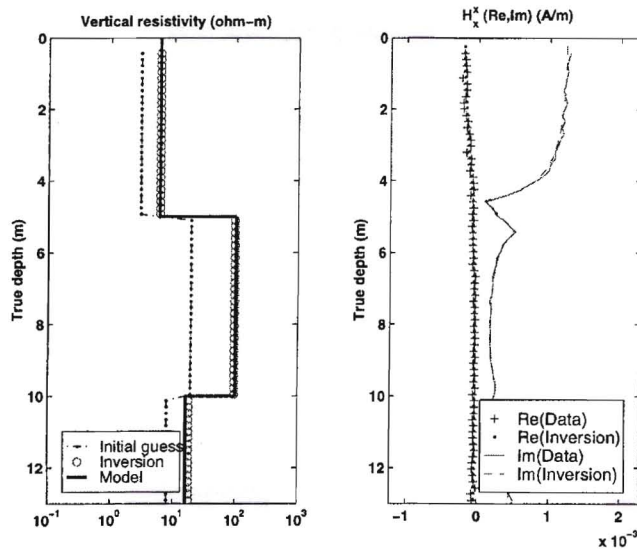


Figure 5: A three layered anisotropic model 2 with a deviated borehole ($\alpha = 30^\circ$). The solid line in the left panel represents a true model of the vertical resistivity. The circles display the inversion result. The dotted-solid line describes the initial approximation. In the right panel we present the real and imaginary parts of the observed and predicted data H_x^2 .

PP

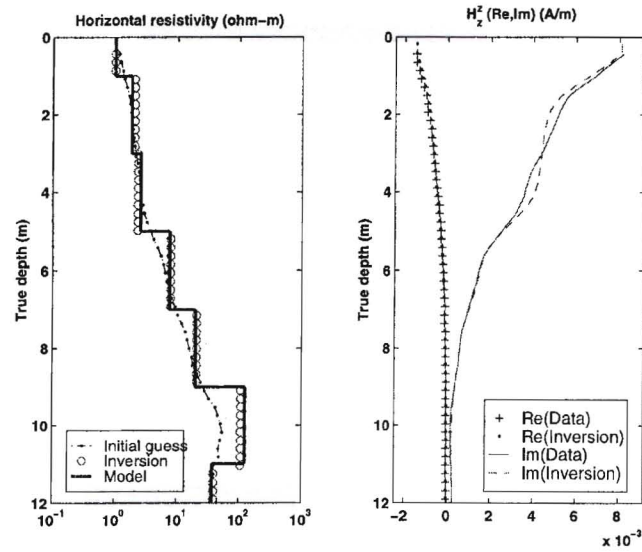


Figure 6: The Baker Atlas benchmark anisotropic model with a deviated borehole ($\alpha = 30^\circ$). The solid line in the left panel represents a true model of the horizontal resistivity. The circles display the inversion result. The dotted-solid line describes the initial approximation. In the right panel we present the real and imaginary parts of the observed and predicted data H_z^z .

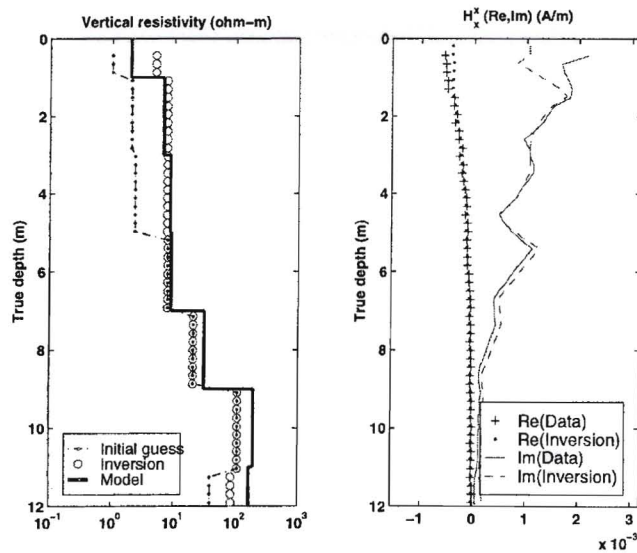
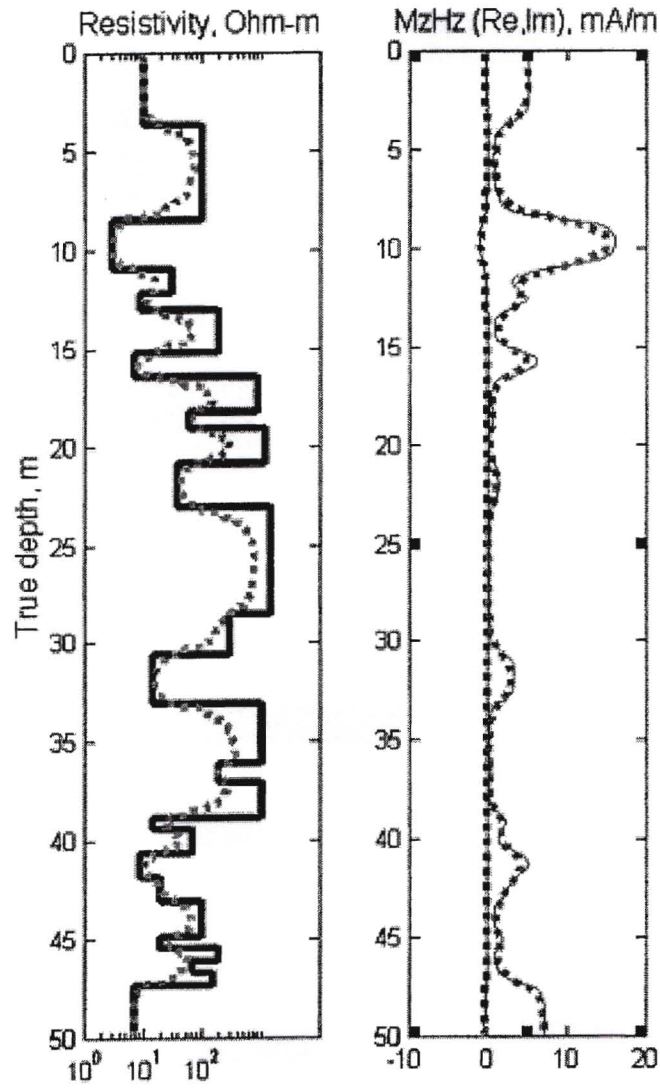


Figure 7: The Baker Atlas benchmark anisotropic model with a deviated borehole ($\alpha = 30^\circ$). The solid line in the left panel represents a true model of the vertical resistivity. The circles display the inversion result. The dotted-solid line describes the initial approximation. In the right panel we present the real and imaginary parts of the observed and predicted data H_x^x .



PP

Figure 8: The horizontal resistivity inversion in the Oklahoma model: the left frame shows the true model (the solid line) and the apparent resistivity model (the initial guess, the dotted line); the right frame presents the real and imaginary parts of the measured synthetic data (the dotted and solid lines) and calculated response (the circle markers). The vertical magnetic field from the vertical magnetic dipole ($MzHz$) is analyzed.

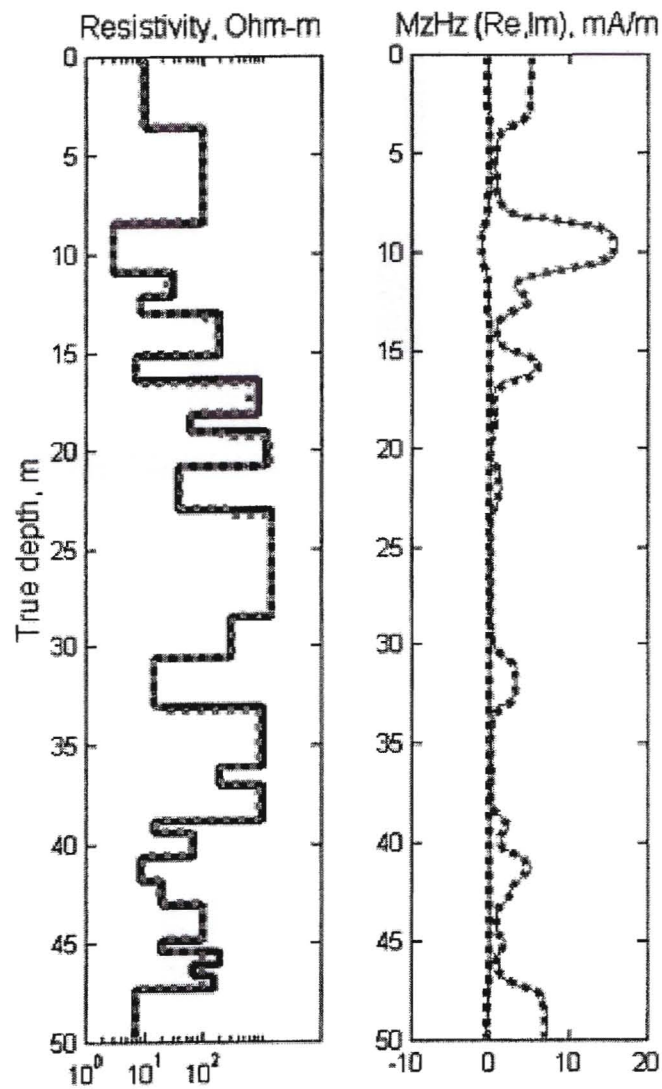
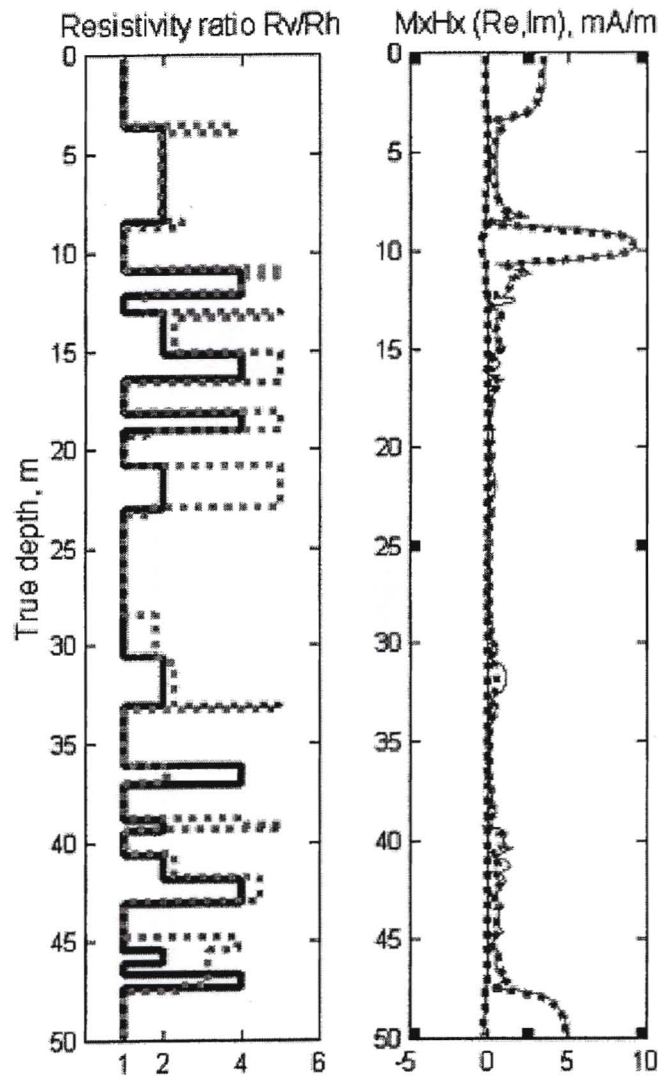


Figure 9: The horizontal resistivity inversion in the Oklahoma model: the left frame shows the true model (the solid line) and the final horizontal resistivity model (the dotted line); the right frame presents the real and imaginary parts of the measured synthetic data (the dotted and solid lines) and predicted response (the circle markers). The vertical magnetic field from the vertical magnetic dipole ($MzHz$) is considered.



PP

Figure 10: The vertical resistivity inversion in the Oklahoma model: the left frame shows the true anisotropy coefficient model (the solid line) and the final anisotropy coefficient model (the dotted line); the right frame presents the real and imaginary parts of the measured synthetic data (the dotted and solid lines) and predicted response (the circle markers). The horizontal magnetic field from the horizontal magnetic dipole ($MxHx$) is considered.